High-Fidelity Conformation of Graphene to SiO_2 Topographic Features

W. G. Cullen,[1,2] M. Yamamoto,[1,2] K. M. Burson,[1,2] J. H. Chen,[1,2] C. Jang,[2] L. Li,[2]
M. S. Fuhrer,[1,2] and E. D. Williams[1,2]

[1]*Materials Research Science and Engineering Center, Department of Physics, University of Maryland, College Park, Maryland 20742-4111, USA*

[2]*Center for Nanophysics and Advanced Materials, Department of Physics, University of Maryland, College Park, Maryland 20742-4111, USA*

(Received 10 August 2010; published 19 November 2010)

High-resolution noncontact atomic force microscopy of SiO_2 reveals previously unresolved roughness at the few-nm length scale, and scanning tunneling microscopy of graphene on SiO_2 shows graphene to be slightly smoother than the supporting SiO_2 substrate. A quantitative energetic analysis explains the observed roughness of graphene on SiO_2 as extrinsic, and a natural result of highly conformal adhesion. Graphene conforms to the substrate down to the smallest features with nearly 99% fidelity, indicating conformal adhesion can be highly effective for strain engineering of graphene.

DOI: 10.1103/PhysRevLett.105.215504 PACS numbers: 61.48.Gh, 68.37.Ef, 68.37.Ps, 68.35.Ct

Graphene's morphology is expected to have a significant impact on its electronic properties [1,2]. Local strain and curvature can introduce effective gauge fields, giving rise to carrier scattering and suppressing weak localization [3]. Engineered strained structures can realize artificial magnetic fields, with the possibility of a quantum Hall state in a zero external field [4,5]. It is therefore important to understand how graphene's morphology is determined by energetics. It has been suggested that freestanding graphene spontaneously adopts a static corrugated morphology [6]. Other researchers have found this explanation unlikely, and have suggested an extrinsic origin for the corrugations observed in freestanding graphene [7]. Regardless, when graphene is placed on a substrate, there is a strong expectation that graphene-substrate adhesion dominates the graphene morphology. This is qualitatively consistent with the observations of flat graphene on atomically flat mica [8], and rough graphene on amorphous SiO_2 [9,10]. However, the understanding of graphene's morphology on a rough substrate is far from settled, and the existing experimental reports [9–11] are at odds with each other. Here we show that the amorphous SiO_2 substrate is in fact much rougher than previously thought, and graphene supported on SiO_2 is slightly smoother than the underlying substrate. Graphene adopts the conformation of the underlying substrate down to the smallest features, consistent with the energetics of adhesion and bending, which indicate that graphene reproduces the substrate topography with nearly 99% fidelity.

In order for graphene to adopt a structure more corrugated than the underlying substrate, it must pay energy costs against both curvature and adhesion. Specifically, the adhesion energy γ of graphene on SiO_2 has been estimated from carbon nanotube experiments [12,13] and self-tensioning of suspended graphene resonators [14] to be $\sim 0.625\ \mathrm{eV/nm^2}$, and has been calculated for graphite/SiO_2 to be $0.5\ \mathrm{eV/nm^2}$ [15]. The energy cost of bending graphene to form ripples is determined by distortion of the C-C bonds with the bending-induced loss of planarity, and the related strain (bond-length changes).

The energy cost of bending graphene sheets [16–18] can be calculated from the uniaxial bending energy/area $E = C\kappa^2/2$ for curvature κ, with $C = 0.85$ eV. Equating the adhesion energy γ to the bending energy then allows a straightforward estimate of the maximum curvature before the graphene "pops free" from the oxide substrate: $1/\kappa = R \geq 0.9$ nm (or for symmetric biaxial bending, where $\kappa_x = \kappa_y$, $R_x \geq 1.3$ nm).

This simple analysis, which suggests that graphene will adhere to the rough morphology of the SiO_2 down to the limit of structural features with a radius of curvature on the order of $R_{\min} \sim 1$ nm will be expanded more quantitatively below, and the basic insight will be shown to hold. Even if the adhesion were an order of magnitude weaker, this conclusion would still hold to feature sizes of $\sim$3 nm.

However, two earlier experiments have been interpreted in terms of an additional thermodynamic driving force which would cause graphene to adopt a nonflat conformation independent of substrate morphology [6,11]. Transmission electron microscopy (TEM) of suspended graphene has shown structural tilts consistent with out-of-plane corrugations of $\sim$1 nm over a spatial extent of 10–25 nm [6]. A recent comparison of SiO_2 roughness measured at low resolution [using conventional atomic force microscopy (AFM)] with SiO_2-supported graphene measured with high resolution (STM) has shown a significantly larger measured roughness for the supported graphene [11]. This result was interpreted as indicating an intrinsic tendency toward graphene corrugation, possibly of the same origin as the corrugation observed in TEM. Here we use high-resolution UHV measurement [19] for both SiO_2 and SiO_2-supported graphene to show that in fact the SiO_2 surface is rougher than previously known at

 © 2010 The American Physical Society

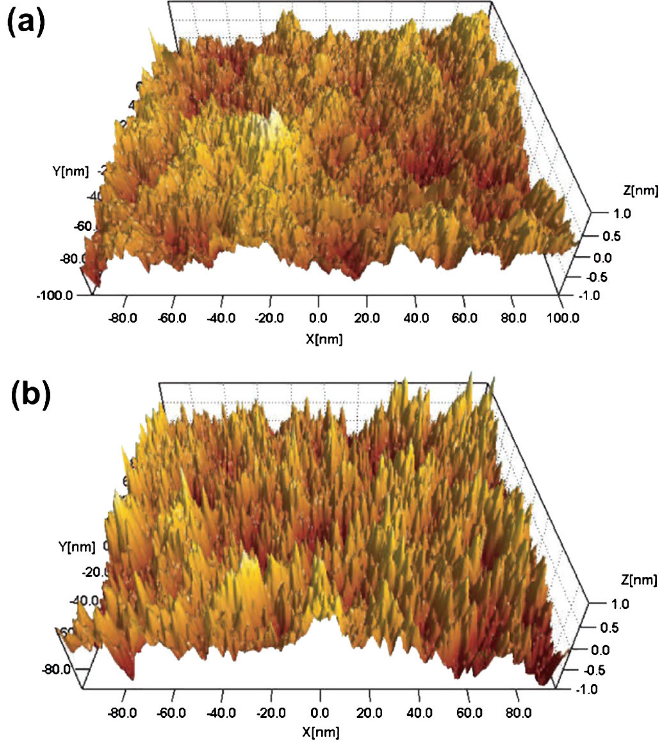

FIG. 1 (color online). (a) STM of SiO_2-supported graphene monolayer (195×178 nm, -305 mV, 41 pA). (b) High-resolution NC-AFM of SiO_2 (195×178 nm, $A = 5$ nm, $\Delta f = -20$ Hz).

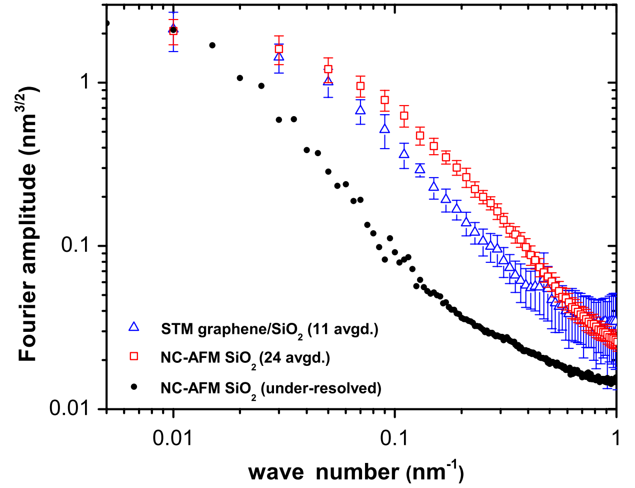

FIG. 2 (color online). Fourier amplitude spectra of: SiO_2 NC-AFM (red squares), monolayer graphene/SiO_2 STM (blue triangles), and under-resolved SiO_2 (black dots). Spectras 1 and 2 were obtained from an averaged data set to establish statistical uncertainty, as discussed in the supporting information. Wave number is defined as wavelength^{-1}.

the smaller lengths scales not accessed in lower resolution measurements. When both the graphene and the supporting substrate are measured with high resolution, the structure of the supported graphene closely matches that of the SiO_2 at all length scales, indicating that the graphene roughness observed is an extrinsic effect due to the SiO_2 substrate; any intrinsic tendency toward corrugation of the graphene is overwhelmed by substrate adhesion.

Figure 1 compares scanned probe images of monolayer graphene on SiO_2 (STM) with bare SiO_2 [high-resolution noncontact atomic force microscopy (NC-AFM)]. The measured rms roughnesses are 0.35 and 0.37 nm, respectively, indicating that graphene is slightly smoother than the SiO_2. Further insight into the structure of graphene on SiO_2 may be gained by examining the Fourier spectra of the height data. Figure 2 shows the Fourier spectra averaged over several images of graphene (STM) and SiO_2 (NC-AFM), for which the images in Fig. 1 are representative. The increased corrugation of the high-resolution measurement of the oxide surface [Fig. 1(b)] is evident in the slightly increased amplitude of the Fourier spectrum (squares in Fig. 2) as compared to the graphene surface [Fig. 1(a) and triangles in Fig. 2]. Also shown for comparison is the Fourier spectrum of a low-resolution measurement of the oxide surface (similar to that reported in Ref. [9]) which preserves the very-long-wavelength structure (wave number < 0.01 nm^{-1}) but clearly misses the structure which is seen by STM. The slightly decreased corrugation of graphene relative to the oxide surface below is expected due to competition between adhesion energy and elastic curvature of the graphene sheet; this competition is discussed quantitatively below.

Understanding the length-scale dependence of the graphene morphology, and the slight decrease in graphene roughness compared with the substrate, requires a more sophisticated analysis adapted from membrane studies. With no applied tension, the Hamiltonian is [20]

$$H = \int \frac{C}{2}[\nabla^2 h(\boldsymbol{r})]^2 + V[h(\boldsymbol{r}) - z_s(\boldsymbol{r})]d^2 r, \qquad (1)$$

where C is the elastic modulus (bending rigidity), $h(\boldsymbol{r})$ is the local height of the membrane, and $z_s(\boldsymbol{r})$ is the local substrate height, both referenced to a flat reference plane ($\boldsymbol{r}$ represents spatial position in the 2D reference plane). We make the simplifying assumption that the adhesion potential can be written as a function of $h(\boldsymbol{r}) - z_s(\boldsymbol{r})$.

The energy is determined by a competition between elastic energy in the graphene sheet and adhesion to the substrate. Significantly, the substrate adhesion term is a function of the local height difference between overlayer and substrate, whereas the elastic terms are directly obtained as functions only of the overlayer topography $h(\boldsymbol{r})$.

We compute the elastic energy (hereafter referred to as the curvature energy E_C) per unit area as

$$E_C = \frac{C}{2}\left\{\frac{1}{A}\int [\nabla^2 h(\boldsymbol{r})]^2 d^2 r\right\}, \qquad (2)$$

where A is the area of the integration domain (statistical distributions of curvature for graphene and SiO_2 are shown in Fig. 3). The quantity in brackets evaluates to

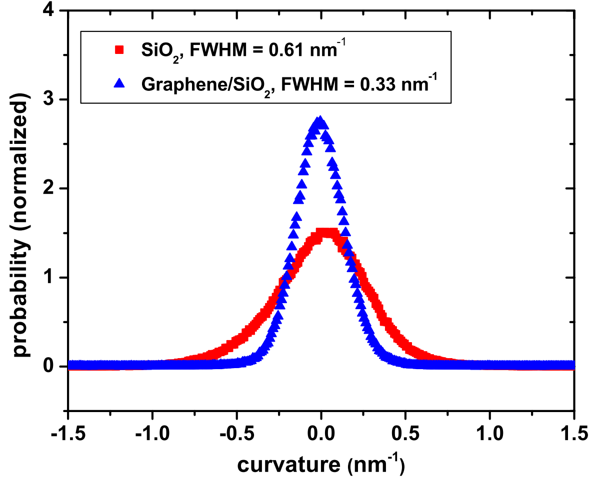

FIG. 3 (color online). Curvature histograms, normalized to unit area, for graphene (narrower distribution) and SiO_2 (broader distribution).

0.078 nm^{-2} for the graphene topography corresponding to the image in Fig. 1(a). Assuming that C is bounded within 0.8–1.4 eV, we obtain 0.031–0.055 eV/nm^2. Now, we may calculate the energy cost of *perfectly* following the substrate by making the substitution $h(\boldsymbol{r}) \rightarrow z_s(\boldsymbol{r})$ in Eq. (2) above. For the SiO_2 topography shown in Fig. 1(b), we obtain 0.092–0.161 eV/nm^2 using the same bounds on C (the quantity in brackets evaluates to 0.23 nm^{-2}). Note that these values are obtained independently of any assumption about the adhesion energy, but their *difference* (avg = 0.084 eV/nm^2) provides a value for the cost of curvature against the adhesion potential; the importance of evaluating this quantity will be shown below.

For gauging the adhesion energy term, we assume that the adhesion potential is harmonic. The calculation in Ref. [15] allows estimation of the harmonic coefficient $v = \partial^2 V/\partial z^2|_{z=h_0} \simeq 56$ eV/nm^4 [19]. Here, h_0 is the distance of the adhesion potential minimum from the substrate surface. The energy cost (per unit area) of deviating from the minimum in the adhesion potential is given by

$$\delta E_A = \frac{v}{2}\left\{\frac{1}{A}\int [h(\boldsymbol{r}) - z_s(\boldsymbol{r})]^2 d^2 r\right\}. \tag{3}$$

We define $\Delta(\boldsymbol{r}) = h(\boldsymbol{r}) - z_s(\boldsymbol{r})$, and see that the quantity in brackets is equivalent to the variance of $\Delta(\boldsymbol{r})$, given in terms of $h(\boldsymbol{r})$ and $z_s(\boldsymbol{r})$ as

$$\sigma_\Delta^2 = \sigma_h^2 + \sigma_{z_s}^2 - 2[\langle h z_s\rangle - \langle h\rangle\langle z_s\rangle], \tag{4}$$

where the final term may be removed by setting either $\langle h\rangle$ or $\langle z_s\rangle = 0$. This expression makes clear that the variance in $\Delta(\boldsymbol{r})$ depends crucially on the degree of correlation between h and z_s. While this correlation is not directly measurable using scanning probe microscopy, it is very instructive to consider its two limits.

In the limit of perfect adhesion (complete correlation), the variances σ_h^2 and $\sigma_{z_s}^2$ are canceled by the correlation term $2\langle h z_s\rangle$, and the variance σ_Δ^2 vanishes [$\Delta(\boldsymbol{r})$ becomes a constant, h_0]. One obtains the full adhesion energy (the complete depth of the potential well) in this case. However, in the uncorrelated limit ($\langle h z_s\rangle = 0$), it is apparent that the variance is very large because there is no cancellation.

The harmonic approximation is valid only for small excursions from the minimum in the potential well, and overestimates the cost of large excursions away from the substrate. Taking an extreme limit of deadhesion $\frac{1}{2} v \sigma_\Delta^2 =$ 0.6 eV/nm^2, we see that this occurs for $\sigma_\Delta = 0.146$ nm, equivalent to an amplitude of 0.207 nm. Thus, graphene with mean amplitude ~0.21 nm, uncorrelated with the SiO_2 substrate, would be essentially deadhered from the substrate. This highlights the key physical concept that significant deviation from the substrate topography is quite costly, even for relatively weak interactions. Graphene which is highly uncorrelated with the underlying substrate would adhere extremely weakly, which is very difficult to reconcile with the known adhesion properties of graphene and carbon nanotubes on SiO_2 [12–14].

In contrast, we now show that the energy balance is satisfied naturally by the highly conformal adhesion proposed here. The previous analysis of curvature energy gives the estimate 0.084 eV/nm^2 for the cost of curvature against the adhesion potential. This implies $\sigma_\Delta^2 =$ 0.003 nm^2 according to Eq. (4) (using $v = 56$ eV/nm^4). A small positive number for σ_Δ^2 is consistent with high (positive) correlation between h and z_s. We obtain $\langle h z_s\rangle / \sigma_h \sigma_{z_s} = 0.99$, indicating an extremely high degree of correlation between graphene and the underlying substrate. The degree of correlation is likely overestimated due to the harmonic approximation for the adhesion potential. Although we cannot image the SiO_2 directly beneath the graphene, our analysis suggests that any topographic feature of the graphene must be the result of an underlying substrate feature.

We used the harmonic approximation as an analytical convenience for quantifying our topographic measurements. However, the description of highly conformal adhesion does not rely on this approximation, and we now discuss our results in the context of recent theories. For an adhesion energy near 0.5–0.6 eV/nm^2 and bending rigidity 1.4–1.5 eV, these unambiguously predict highly conformal adhesion [21–23]. In Ref. [22], the graphene-SiO_2 adhesion potential is described analytically by a Lennard-Jones pair potential, while in Ref. [21] a similar pair potential is used but with Monte Carlo integration over substrate atoms. Both are parametrized in terms of the ratio A_s/λ, with the substrate modeled as a single-frequency sinusoidal corrugation with amplitude A_s and wavelength λ. The SiO_2 topography exhibits power-law scaling with a correlation length ~10 nm; associating the full $\sigma_{\rm rms} =$ 0.37 nm with $\lambda \sim 10$ nm, we obtain $A_s/\lambda \sim 1/20$. The

adhesion transitions predicted in Refs. [21,22] occur only in the limit of much larger A_s/λ or much weaker adhesion, and both predict high conformation, with ratio $A_g/A_s > 0.9$ [A_g is the sinusoidal amplitude of graphene (g)]. From our $\sigma_{\rm rms}$ values, $A_g/A_s = 0.95$.

Conformal graphene adhesion is further predicted by Ref. [23]; it is shown that for a periodic sinusoidal substrate profile, deadhesion will occur in a series of transitions where first the membrane breaks loose from every other trough, then every two out of three troughs, and so on. In the zero-tension limit, these transitions are governed solely by the dimensionless parameter α, where $\alpha = (\kappa_{\rm eq}/\kappa_s)^{1/2}$. Here, $\kappa_{\rm eq} = (2\gamma/C)^{1/2}$ with adhesion energy γ and bending rigidity C as above. κ_s is the geometrical curvature of the substrate. A perfectly conforming ground state is predicted for $\alpha \geq 0.86$. Making conservative estimates $\gamma = 0.5$ eV/nm^2 and $C = 1.4$ eV, the transition from perfect conformation occurs at substrate curvature $\kappa_s = 1.14$ nm^{-1}. Figure 3 shows a histogram of surface curvature obtained from high-resolution NC-AFM measurement of SiO_2, where it is apparent less than 0.1% of the surface has curvature exceeding 1.0 nm^{-1}.

Our preceding arguments have demonstrated that highly conformal adhesion to the SiO_2 substrate accounts for the observed graphene topography. This is primarily because the curvature energy scale set by the corrugation of SiO_2 is modest compared to that of the adhesion potential. ''Intrinsic'' rippling of graphene on SiO_2 is physically unrealistic due to the overwhelming energy cost of deviating from the local minimum in $V(z)$. A recent calculation for isolated graphene finds the statically rippled structure energetically favored by 0.0005 eV/nm^2 [24], miniscule in comparison to the energy scale set by adhesion. Further, we are unaware of any theory which predicts an *intrinsic* rippling of graphene when supported on a substrate, as additional energy would be required to offset the cost against bending energy and adhesion. A buckling instability does exist in the presence of external compressive strain [22], however.

We have shown that the corrugation observed for graphene on SiO_2 using STM is due to a higher corrugation of SiO_2, unresolved in previous AFM measurements. This presents a natural, intuitive description of exfoliated graphene topography based on established membrane physics. Our measurements agree with predictions of three different theoretical models which use different parametrizations of the adhesion potential [21–23]. Careful consideration of the energy balance between bending rigidity and substrate adhesion shows that highly conformal adhesion gives a consistent description, whereas intrinsic rippling of graphene severely violates this balance. This interpretation is fully consistent with recent measurements of graphene exfoliated onto mica, which was found to be flat within 25 pm [8]. Even though our measurements of SiO_2 reveal higher corrugation than previously measured, the roughness is insufficient to induce the interesting structural transitions predicted by recent theories. Exploration of these issues, either by tailored substrates or chemical modification of graphene elasticity will provide interesting experiments for future work.

This work has been supported by the University of Maryland NSF-MRSEC under Grant No. DMR 05-20471 with supplemental funding from NRI, and the U.S. ONR MURI. MRSEC Shared Experimental Facilities were used in this work. Additional infrastructure support provided by the UMD NanoCenter and CNAM. We would like to thank Nacional de Grafite for providing samples of natural graphite.

[1] M. I. Katsnelson and A. K. Geim, Phil. Trans. R. Soc. A **366**, 195 (2008).
[2] E. Kim and A. H. Castro Neto, Europhys. Lett. **84**, 57 007 (2008).
[3] S. V. Morozov *et al.*, Phys. Rev. Lett. **97**, 016801 (2006).
[4] F. Guinea, M. I. Katsnelson, and A. K. Geim, Nature Phys. **6**, 30 (2010).
[5] V. M. Pereira and A. H. Castro Neto, Phys. Rev. Lett. **103**, 046801 (2009).
[6] J. Meyer *et al.*, Nature (London) **446**, 60 (2007).
[7] R. C. Thompson-Flagg, M. J. B. Moura, and M. Marder, Europhys. Lett. **85**, 46002 (2009).
[8] C. H. Lui *et al.*, Nature (London) **462**, 339 (2009).
[9] M. Ishigami *et al.*, Nano Lett. **7**, 1643 (2007).
[10] E. Stolyarova *et al.*, Proc. Natl. Acad. Sci. U.S.A. **104**, 9209 (2007).
[11] V. Geringer *et al.*, Phys. Rev. Lett. **102**, 076102 (2009).
[12] R. S. Ruoff *et al.*, Nature (London) **364**, 514 (1993).
[13] T. Hertel, R. E. Walkup, and P. Avouris, Phys. Rev. B **58**, 13 870 (1998).
[14] J. S. Bunch *et al.*, Nano Lett. **8**, 2458 (2008).
[15] D. Henry, C. Lukey, E. Evans, and I. Yarovsky, Mol. Simul. **31**, 449 (2005).
[16] D. H. Robertson, D. W. Brenner, and J. W. Mintmire, Phys. Rev. B **45**, 12 592 (1992).
[17] B. I. Yakobson, C. J. Brabec, and J. Bernholc, Phys. Rev. Lett. **76**, 2511 (1996).
[18] A. Incze, A. Pasturel, and P. Peyla, Phys. Rev. B **70**, 212103 (2004).
[19] See supplementary material at http://link.aps.org/supplemental/10.1103/PhysRevLett.105.215504 for a pdf file including full experimental details.
[20] G. Palasantzas and G. Backx, Phys. Rev. B **54**, 8213 (1996).
[21] T. Li and Z. Zhang, J. Phys. D **43**, 075303 (2010).
[22] Z. H. Aitken and R. Huang, J. Appl. Phys. **107**, 123531 (2010).
[23] O. Pierre-Louis, Phys. Rev. E **78**, 021603 (2008).
[24] N. Abedpour, R. Asgari, and M. R. R. Tabar, Phys. Rev. Lett. **104**, 196804 (2010).